Title
Stereotactic Charged-Particle Radiosurgery: Clinical Results of Treatment of 1200 Patients with Intracranial Arteriovenous Malformations and Pituitary Disorders

Journal
Clinical Neurosurgery, 38

Authors
Fabrikant, J.I.
Levy, R.P.
Steinberg, G.K.
et al.

Publication Date
1992

LBL-30992
Preprint

Lawrence Berkeley Laboratory
UNIVERSITY OF CALIFORNIA

Submitted to Clinical Neurosurgery

Stereotactic Charged-Particle Radiosurgery: Clinical Results of Treatment of 1200 Patients with Intracranial Arteriovenous Malformations and Pituitary Disorders

J.I. Fabrikant, R.P. Levy, G.K. Steinberg, M.H. Phillips, K.A. Frankel, and G.D. Silverberg

October 1990

Donner Laboratory

Biology & Medicine Division

Prepared for the U.S. Department of Energy under Contract Number DE-AC03-76SF00098

STEREOTACTIC CHARGED-PARTICLE RADIOSURGERY: CLINICAL RESULTS OF TREATMENT OF 1200 PATIENTS WITH INTRACRANIAL ARTERIOVENOUS MALFORMATIONS AND PITUITARY DISORDERS[1]

Jacob I. Fabrikant, M.D., Ph.D.,[*] Richard P. Levy, M.D.,[†] Gary K. Steinberg, M.D., Ph.D.,[‡] Mark H. Phillips, Ph.D.,[§] Kenneth A. Frankel, Ph.D.,[Φ] and Gerald D. Silverberg, M.D.[‖]

[*] Professor of Radiology, University of California, San Francisco and Berkeley; Medical Scientist and Senior Scientist, Donner Pavilion and Donner Laboratory, Division of Research Medicine and Radiation Biophysics, Lawrence Berkeley Laboratory, University of California, Berkeley, California

[†] Assistant Adjunct Professor of Radiology, University of California, San Francisco; Medical Scientist and Staff Scientist, Donner Pavilion and Donner Laboratory, Division of Research Medicine and Radiation Biophysics, Lawrence Berkeley Laboratory, University of California, Berkeley, California

[‡] Assistant Professor of Neurosurgery, Stanford University School of Medicine, Stanford, California

[§] Assistant Adjunct Professor of Radiology, University of California, San Francisco; Staff Scientist, Donner Pavilion and Donner Laboratory, Division of Research Medicine and Radiation Biophysics, Lawrence Berkeley Laboratory, University of California, Berkeley, California

[Φ] Assistant Adjunct Professor of Radiology, University of California, San Francisco; Staff Scientist, Donner Pavilion and Donner Laboratory, Division of Research Medicine and Radiation Biophysics, Lawrence Berkeley Laboratory, University of California, Berkeley, California

[‖] Professor of Neurosurgery, Stanford University School of Medicine, Stanford, California

Direct correspondence to:

Jacob I. Fabrikant, M.D., Ph.D.
Donner Pavilion and Donner Laboratory
University of California at Berkeley
Berkeley, California 94720
Telephone: (415) 486-6118

Running title: Stereotactic Charged-Particle Radiosurgery

---

[1] This work was supported by the Director, Office of Energy Research, Office of Health and Environmental Research, of the U.S. Department of Energy under Contract No. DE-AC03-76SF00098.

INTRODUCTION

The first stereotactic radiosurgical procedures using accelerated charged particles in clinical patients were developed in 1954 at the Lawrence Radiation Laboratory at the University of California at Berkeley [17, 41-43]. Treatment was performed for pituitary hormone suppression in patients with metastatic breast carcinoma. Since then, more than 6,000 neurosurgical patients world-wide have been treated with stereotactic charged-particle radiosurgery of the brain for various nonmalignant and malignant disorders, primarily for pituitary suppression in patients with metastatic breast and prostate cancer and proliferative diabetic retinopathy, pituitary adenomas, intracranial vascular malformations, and selected intracranial tumors, including gliomas, meningiomas, acoustic neuromas, and pinealomas [21]. This report will be limited to heavy-charged-particle (helium-ion) radiosurgery and our experience at the University of California at Berkeley [3-7, 17-23, 39]. This experience, particularly for the treatment of pituitary tumors and intracranial arteriovenous malformations, has been paralleled to some extent by the clinical experience with proton-beam radiosurgery in Boston [10-15] and in the Soviet Union [16, 24, 30-35].

The physical properties of charged-particle beams have certain advantages over high-energy photons (X and gamma rays) for radiosurgery and radiotherapy, and this is particularly the case for stereotactic radiosurgery of intracranial disorders [21, 37]. These characteristics include a well-defined range in tissue, a low entry dose (plateau region), an increased dose at depth (Bragg ionization peak), very sharp lateral edges, and rapid dose falloff distally with little or no exit dose (Fig. 1) [5, 21, 27, 28]. With the use of precision patient immobilization techniques, beam collimation, beam-shaping apertures, modulation of the width of the Bragg peak, and tissue compensation, beams of accelerated charged particles may be stereotactically directed to place a high dose of radiation preferentially within the limits of deeply-located intracranial targets while protecting adjacent normal neural structures [3-7, 20, 21].

PITUITARY TUMORS

Biological Rationale

Based on extensive biological studies and experience with protracted dose schedules from clinical radiotherapy, Lawrence and his colleagues developed stereotactic radiosurgery of pituitary tumors and related neuroendocrine disorders at Donner Laboratory [17-19, 21-23, 40-43]. With high-energy particle beams it was possible to overcome the relative insensitivity of the pituitary gland to externally-delivered X or gamma radiotherapy without irradiating large volumes of surrounding normal brain tissue [21, 40]. It was important to maximize the dose to the pituitary gland while protecting the adjacent critical structures (e.g., optic chiasm, hypothalamus, and brain stem), and to minimize the dose to the temporal lobes of the brain and the cranial nerves [18, 21, 40].

Histological observations have demonstrated that more than 95 percent of the pituitary cells can be destroyed and replaced with fibrous tissue within several months following helium-ion beam radiation doses as high as 180 to 220 Gy delivered over a two to three week period [40, 44]. At lesser doses delivered over shorter periods, the histopathological changes depended on the dose to the periphery of the gland, where the viable, hormone-secreting cells are located. Surviving cells from the center of the gland tend to migrate to the periphery where the blood supply is best. In acromegaly, Cushing's disease, Nelson's syndrome and prolactinomas, the therapeutic goal has been to destroy or inhibit the growth of the pituitary tumor and control hormone hypersecretion while preserving a functional rim of tissue with normal hormone-secreting capacity, and minimizing neurological injury [18, 21-23].

Treatment Procedure

Using X-ray localization techniques, beam-shaping, brass collimators, and heavy-ion beam autoradiographs, the beam was centered precisely on the pituitary fossa (Fig. 2) [21, 40]. The placement of the beam within the immobilized head in the stereotactic frame is accurate to within 0.3 mm., and this accuracy is maintained while the head is rotated in pendulum motion around a horizontal axis and during multiport procedures while the patient's body is positioned at multiple angles around a vertical axis (Fig. 3) [21, 40]. Treatment was delivered in six to eight fractions over a two to three week interval in the first few years of the clinical research program, and in three or four fractions over five days, subsequently. Doses are high, 30 to 150 Gy, in order to overcome the radioresistance of the pituitary gland: for acromegaly, 30 to 50 Gy, four fractions in five days; for Cushing's disease, Nelson's syndrome, and prolactin-secreting tumors, 50 to 150 Gy in four daily fractions. The doses to the adjacent cranial nerves and temporal lobes are considered to be limiting factors rather than the dose to the pituitary gland; the medial aspect of the temporal lobe received 36 Gy during longer courses of therapy, and 30 Gy during shorter courses. The optimal treatment procedure is designed so that the optic chiasm, hypothalamus, and outer portions of the sphenoid sinus receive less than ten percent of the nominal dose to the pituitary [18, 21-23, 40].

Dose Distribution

Currently, the typical isodose distribution for the plateau-region irradiation procedure (Fig. 2) follows the contour of the pituitary gland based on computerized tomography (CT) and magnetic resonance image (MRI) correlation for treatment planning. The dose decreases rapidly in the arteroposterior direction and toward the optic chiasm, and more slowly toward the temporal lobes [21, 40]. High-energy collimated helium-ion beams (230 MeV/u) were used in treating over 800 pituitary patients; the plateau region of the beam passed through the head without being seriously attenuated. The nominal dose, that is, the maximum absorbed dose delivered to the geometric center of the pituitary, ranged from 30 Gy to 150 Gy, depending on a number of factors, and is the sum total of beam doses passing through the external ion chamber integrator. Biologically, the absorbed dose at the peripheral edges of the gland is about 50% of the nominal dose. The effectiveness of the absorbed dose is further modified due to cellular repair between dose fractions. In the three-dimensional isodose distribution reconstruction, stereotactic helium-ion radiosurgery proved very much better than the isodose curves obtained with conventional photon radiation, which usually cannot avoid sensitive adjacent neural structures, e.g., the optic chiasm. The recent introduction of stereotactic helium-ion radiosurgery with the unmodified Bragg ionization peak results in a vastly superior isodose distribution; this technique has special application for the treatment of pituitary microadenomas or eccentrically-located tumor recurrences now demonstrated on high-resolution, multiplanar MRI scans (Figs. 4 and 5) [21].

Clinical Outcome

Over a 30-year period, 840 pituitary patients with a variety of pituitary or neuroendocrine disorders were treated with stereotactic heavy-charged-particle (helium-ion) radiosurgery. Analysis of results in 799 patients, including 467 with pituitary tumors, 157 with metastatic breast cancer, and 169 with diabetic retinopathy, indicate that the clinical outcomes have been excellent [23]. In acromegaly, marked clinical, biochemical and metabolic improvement was observed in most patients within the first year; the mean growth hormone level decreased nearly 70 percent within one year, continued to decrease thereafter, and normal levels were maintained during more than ten years of followup [18, 19, 23]. Cushing's disease has been treated successfully; mean basal cortisol levels and dexamethasone suppression testing returned to normal values within one year after treatment, and remained normal during more than ten years of followup [19, 23]. All Nelson's syndrome patients exhibited marked decrease in ACTH levels, but rarely to normal levels [19, 23]. In patients with prolactin-secreting tumors, serum prolactin levels were successfully reduced to normal or near-normal levels within one year [23]. Variable degrees of hypopituitarism developed in about a third of the patients; endocrine deficiencies were rapidly corrected in most patients with appropriate hormone replacement therapy [23]. The incidence of CNS complications, including focal temporal lobe necrosis and cranial nerve injury, was less than one percent. This complication rate is less than for photon therapy and for transsphenoidal hypophysectomy [23].

INTRACRANIAL ARTERIOVENOUS MALFORMATIONS

We have developed an advanced method of stereotactic heavy-charged-particle Bragg peak radiosurgery for treatment of surgically inaccessible intracranial AVMs lying deep within the brain [3-7, 20, 21, 27, 28, 36, 38, 39]. We now know that the radiobiological basis for obliteration of the vascular shunts involves radiation injury to the endothelial cell populations and their supporting architecture, intimal cell proliferation, hyaline degeneration of the media, thrombosis and fibrosis [3, 5]. The precision of our treatment planning and beam delivery system assures improved dose localization and dose distribution of the Bragg ionization peak within the AVM with little or no neurovascular or parenchymal injury to adjacent vital neural structures. To date, we have treated approximately 400 patients with inoperable intracranial vascular malformations, including 50 patients aged 18 years or younger and 42 patients with angiographically-occult vascular malformations. Based on evaluation using cerebral angiography, CT and MRI scanning, and extensive clinical neurological follow-up, stereotactic heavy-charged-particle Bragg peak radiosurgery obliterates intracranial AVMs and protects against further brain hemorrhage, with reduced morbidity and no treatment-associated mortality. The incidence of complications is low, and includes white matter changes and vasculopathy [21, 39]. We consider the method appropriate only in selected patients, and patient selection is constrained by specifically-defined guidelines in patient protocols.

Dose Distribution

In the standard configuration, the helium-ion beam line has a 14.1 to 14.5 cm range to the Bragg ionization peak, with very sharply delimited lateral and distal borders (Fig. 1) [5, 27, 28]. In clinical applications, the range of the charged-particle beam is decreased to the desired value, and the beam is shaped to conform to the configuration of the AVM and to any diameter from less than 6 mm to over 60 mm [20, 21]. The maximum dose in the unmodified Bragg peak within the brain is approximately two to three times greater than the plateau or entrance dose at the skin; there is no exit dose (Fig. 1) [5, 21, 27, 28]. The unmodulated Bragg peak width is only a few millimeters, but can be spread out to any desired width to approximately 35 mm or more using specially-designed filters (Fig. 3). The primary advantage of narrow beams of heavy-charged-particles in radiosurgical treatment deep within the brain is the ability to confine the dose to a discrete volume of tissue while protecting adjacent critical neural structures [25, 37]. The improved physical dose distributions are made possible by the relatively small amount of multiple scattering and range straggling and by the rapid fall-off of dose with depth beyond the Bragg peak. These same physical characteristics require a stringently accurate assessment of, and compensation for, inhomogeneities in the tissue in order to accomplish precision radiosurgery with focal charged-particle beams [3, 5, 21].

The dose to the central axis of the AVM, the aperture size and collimation, the number of ports, and the beam angles for delivery and the range and modulation of the Bragg peak all determine the isodose contour configurations. Currently, total doses up to 25 GyE (physical dose x relative biological effectiveness of the charged-particle Bragg ionization peak) are delivered to treatment volumes ranging from about 100 mm^3 to 70,000 mm^3. Initially, doses to 35 and 45 GyE were used in the dose searching protocol. At present, however, the optimal dose inducing obliteration of the AVM with the smallest risk of neurological sequelae depends on a number of factors and appears to be in the range of 25 to 15 GyE, using the helium-ion Bragg ionization peak (RBE of 1.3) [1, 5, 39]. Dose selection depends on the size, shape and location of the AVM within the brain and a number of other factors, including the volume of normal brain that must be traversed by the plateau portion of the charged-particle beam.

Treatment Planning

The aim of the radiosurgical procedure is to use focal charged-particle beams to irradiate the main arterial feeders and abnormal shunting vessels of the malformation proper and to include, as completely as possible, the whole cluster of pathological shunting vasculature within the radiation field. An optimal treatment plan requires that the entire arterial phase of the AVM can be covered by a sufficient and uniform radiation dose [5, 20, 21, 39]. Treatment with stereotactically-directed heavy-charged-particle beams is based on computer-assisted treatment planning of the dose distribution (isodose contour display), calculated for each individual patient from the stereotactic cerebral angiograms and stereotactic CT scans and MRI images [3-7, 20, 21, 36, 38]. The anatomic basis for this treatment planning procedure integrates information from the stereotactic neuroradiological procedures; the data are used for target contouring and conversion to relative stopping powers for conforming the Bragg ionization peak to the three-dimensional contour of the target volume within the brain. Beam modulation, together with multiple entry angles and beamports, shaped apertures, and tissue compensators are chosen to conform the high dose Bragg peak to the contoured target of the AVM within the brain while protecting adjacent critical neural structures [5, 20, 21]. Head immobilization is achieved with the individualized thermoplastic immobilization mask and stereotactic frame used for all neuroradiological procedures and which serve as integral components of the system's patient-positioning apparatus, the Irradiation Stereotactic Apparatus for Humans (ISAH) (Fig. 6) [5, 26, 29]. The patient-positioning system assures precise immobilization for optimal beam delivery and localization of the helium-ion beam path in relation to the stereotactically-determined isocenter [5, 21, 29].

The average treatment volume for most patients ranges from 1,500 to 16,000 mm^3. Treatment generally occurs through three to seven entry angles, most frequently four noncoplanar beams confined to one side of the brain, and is delivered daily in one or two fractions, depending on the treatment volume (e.g., in one day if the volume is 4,000 mm^3 or less, in two days if larger) and the volume of normal brain tissue traversed by the plateau beams. The dose to the critical normal brain structures adjacent to the AVM is considerably less than the dose to the target volume because fall-off of the central dose occurs within 4 to 6 mm (within 2 to 3 mm at the Bevatron), and is within 2 to 3 mm along the lateral margins of the helium-ion beam (Fig. 1) [5]. Figures 7 and 8 are examples of treatment plans illustrating the isodose contours for stereotactic heavy-charged-particle Bragg peak radiosurgery in patients with cerebral AVMs. In Figure 7, the AVM is quite small, only 300 mm^3, but lies in a critical site within the brain stem; it is defined by the inner ring of white dots on the treatment-plan CT scan. The helium-ion beam was collimated by an 8.5 x 11.5 mm elliptical brass aperture; treatment was carried out using four noncoplanar ports in one day to a dose of 25 GyE. Figure 8 illustrates the treatment plan for a large right frontal AVM, defined by the inner ring of white dots; the 90 percent isodose contour lies on the edge of the AVM, and five beamports were used to deliver a dose of 28 GyE to a volume of 26,000 mm^3 in two daily fractions.

Clinical and Neuroradiological Outcomes

The clinical objectives are to achieve changes in the intracerebral hemodynamic condition, resulting in: reduction or elimination of brain hemorrhages with their associated morbidity and mortality; decrease in progressive or fixed neurological deficits; lowered frequency of seizures; and fewer subjective complaints, including a decreased frequency and intensity of vascular headaches. Nearly all of our 400 patients thus far treated have received clinical and neuroradiological follow-up, and extended review and evaluation has now been carried out to ten years on a regular basis. We use the Drake clinical grading system [2, 39]; in over 90 percent of our patients an excellent or good clinical outcome has been achieved. Of those patients followed for two or more years, therapy leading to obliteration of an AVM has improved seizures, headaches, and neurological deficit in a high percentage of patients [39]. Thus far, preliminary observations indicate that our clinical objectives are being achieved [3-7, 20, 39].

Cerebral angiography shows changes in cerebral vessels at intervals following radiosurgery. Hemodynamic changes are manifested by a decrease in blood flow rate and volume through the pathological cluster of the AVM shunts and a decrease in size of the feeding arteries, shunts, and draining veins. Anatomical changes include a progressive decrease in size of the AVM until stabilization or total obliteration of the lesion occurs. The hemodynamic changes occur successively and are usually observed before the anatomical changes. Neuroradiological follow-up to the end of 1989 in 230 patients indicates that for complete obliteration three years after treatment, the incidences are: 90-95 percent for treatment volumes <4,000 mm^3; 90-95 percent for volumes between 4,000 mm^3 and 14,000 mm^3, and 60-70 percent for volumes > 14,000 mm^3; for all volumes (up to 70,000 mm^3), it has been approximately 80-85 percent [5, 20, 21, 39]. Occlusion occurs most completely in the high-dose (30 to 45 GyE) group of patients. The intermediate dose (24 to 28 GyE) also proved to be quite effective (Fig. 9). Preliminary results with the lowest-dose group (11.5 to 20 GyE) are encouraging at the 3-year-followup interval, but thus far the numbers of patients in this group are too small to draw firm conclusions. Following complete AVM obliteration, which usually occurs between 7 and 34 months after treatment, we have not seen subsequent angiographic reappearance of the AVM, even when prior embolization was performed [39].

Major complications occurred in 12 percent of patients, and include white matter changes and vasculopathies, leading to transient or permanent neurological deficits [39]. All these complications occurred in the initial stage of the dose-searching protocol, before the maximum dose of radiation was reduced to 25 GyE. In addition, hemorrhage occurred in about ten percent of patients from residual malformations after treatment; most of these patients had bled prior to radiosurgery [39].

Positron emission tomography (PET) provides a valuable quantitative method for examining changes in tissue glucose metabolism and blood flow dynamics before and after stereotactic radiosurgery [5]. Figure 10 illustrates a patient with a left cerebral AVM and its regional tissue metabolism using ^{18}fluorodeoxyglucose (^{18}FDG) and PET scanning with the Donner Laboratory 600-crystal positron tomography unit. The AVM is seen extending into the left thalamus and deep white matter of the left cerebral hemisphere. Following radiosurgery, the pronounced white matter changes observed on MRI revealed vasogenic edema associated with a small region of radiation necrosis. Decreased cortical metabolism in the irradiated hemisphere is demonstrated by diminished ^{18}FDG uptake.

From the longest follow-up available we can conclude that by stereotactically-directed, focal-beam charged-particle Bragg peak irradiation of the feeding and abnormal shunts, total and irreversible angiographic obliteration of life-threatening, deep-seated, surgically-inaccessible intracranial AVMs is possible in a large number of patients, and protection against recurrent hemorrhage with reduced morbidity and mortality occurs in about 80 to 85 percent of patients. The rate of serious complications is relatively low, approximately 12 percent, particularly when compared with the natural history of such lesions, the potential for spontaneous intracranial hemorrhage with profound neurological sequelae in untreated patients, and the outcomes of conventional surgery for these difficult lesions [2, 8, 9].

UNIVERSITY OF CALIFORNIA AT BERKELEY -STANFORD UNIVERSITY MEDICAL CENTER CLINICAL TRIAL

Our recent report on the detailed clinical and neuroradiological follow-up in 86 consecutive patients treated for angiographically-demonstrable intracranial arteriovenous malformations provides an evaluation that is representative of the entire series [39]. All patients were symptomatic with surgically-inaccessible cerebral malformations; they were treated with stereotactic helium-ion Bragg peak radiosurgery with doses ranging from 11 GyE to 45 GyE to treatment volumes of 300 mm^3 to 70,000 mm^3. The rate of complete angiographic obliteration two years after radiosurgery (as a function of angiographically-determined volume [39]) was 94 percent for AVMs less than 4,000 mm^3, 75 percent for those 4,000 mm^3 to 25,000 mm^3, and 39 percent for those larger than 25,000 mm^3. After three years, the rates increased to 100, 95 and 70 percent, respectively, with an overall obliteration rate in this subgroup of 92 percent. Severe neurological complications occurred in 12 percent of patients, the majority of whom experienced permanent neurological deficits; all clinical complications occurred in the high-dose patient group in the initial phase of the dose-searching protocol, before the doses were reduced to $\leq$25 GyE. Hemorrhage occurred in 12 percent of patients from residual AVMs between four and 34 months following irradiation. In 94 percent of patients, an excellent or good clinical outcome resulted; seizures and headaches were improved in 63 percent and 68 percent of patients, respectively.

CONCLUSIONS

Based on evaluation using cerebral angiography, CT and MRI scanning, together with extensive neurological workup, it currently appears that stereotactic heavy-charged-particle Bragg peak radiosurgery obliterates high-flow intracranial AVMs and protects against further brain hemorrhage with reduced morbidity and no treatment-associated mortality. We have now treated approximately 400 patients with symptomatic surgically-inaccessible cerebral AVMs with excellent or good clinical outcomes, and with obliteration of some 80-85 percent of all lesions. The current procedure still has two major disadvantages: the prolonged latent period during which time the patient remains at risk of hemorrhage from residual shunts, and the relatively ~~low incidence of~~ small risk of serious neurological complications.

Although dose reduction has successfully lowered the complication rate, it appears that it decreases the obliteration rate and prolongs the latency interval prior to complete obliteration; this is particularly evident in the patient group with large-sized AVMs. Accordingly, we are continuing to evaluate dose-searching protocols to determine the optimal dose for each patient, depending on size, shape and location of the AVM, in order to improve clinical outcomes with the least rates of complications and hemorrhage. The multistage approach we have recently introduced to reduce malformation size and decrease blood flow prior to radiosurgery includes endovascular embolization and partial surgical resection; this may be useful in treating selected large malformations, since this group generally has the lowest obliteration rate and the highest complication rate. Overall, the vascular obliteration rates are relatively high in this high-risk patient population, and the serious complications thus far encountered may be considered acceptable in view of the potential for spontaneous intracranial hemorrhage and profound neurological sequelae, morbidity and mortality associated with the natural history of this disease in untreated patients, and in whom the potential surgical risk of morbidity and mortality is considered unacceptably high [8, 9, 39].

ACKNOWLEDGEMENTS

The authors wish to thank Professors J.H. Lawrence, C.A. Tobias, E.L. Alpen, R.N. Kjellberg, Ye. I. Minakova, B.A. Konnov, T.F. Budinger, and G.D. Silverberg, Drs. E.H. Lo, P. Valk, Mr. F.Y.S. Chuang, and Ms. M. Foster for providing research material and permission to describe their clinical and basic research, for assistance, and for many helpful discussions. The authors thank Mr. J. McCarthy and Mr. A. Linard for assistance with preparation of the manuscript.

REFERENCES

1. Blakely EA, Ngo FQH, Curtis SB, et al: Heavy-ion radiobiology: Cellular studies. *In* Lett JT (ed): Advances in Radiation Biology, vol 11, New York, Academic Press, 1984, pp 295-389

2. Drake CG: Cerebral arteriovenous malformations: Considerations for and experience with surgical treatment in 166 cases. Clin Neurosurg 26:145-208, 1979

3. Fabrikant JI, Frankel KA, Phillips MH, et al: Stereotactic heavy charged-particle Bragg peak radiosurgery for intracranial arteriovenous malformations. *In* Edwards MSB, Hoffman HJ (eds): Cerebral Vascular Diseases of Children and Adolescents. Baltimore, Williams & Wilkins, 1989, pp 389-409

4. Fabrikant JI, Levy RP, Frankel KA, et al: Stereotactic helium-ion radiosurgery for the treatment of intracranial vascular malformations. *In* International Workshop on Proton and Narrow Photon Beam Therapy, Oulu, Finland, University of Oulu Printing Center, 1989, pp 33-37

5. Fabrikant JI, Levy RP, Steinberg GK, et al: Stereotactic heavy-charged-particle radiosurgery for the treatment of intracranial vascular malformations. Neurosurg Clin North Am, in press

6. Fabrikant JI, Lyman JT, Frankel KA: Heavy charged-particle Bragg peak radiosurgery for intracranial vascular disorders. Radiat Res [Suppl] 104:S244-S258, 1985

7. Fabrikant JI, Lyman JT, Hosobuchi Y: Stereotactic heavy-ion Bragg peak radiosurgery: Method for treatment of deep arteriovenous malformations. Br J Radiol 57:479-490, 1984

8. Fults D, Kelly DL Jr: Natural history of arteriovenous malformations of the brain; a clinical study. Neurosurgery 15:658-662, 1984.

9. Heros RM, Tu Y-K: Is surgical therapy needed for unruptured arteriovenous malformations? Neurology 37:279-286, 1987

10. Kjellberg RN: Stereotactic Bragg peak proton beam radiosurgery for cerebral arteriovenous malformations. Ann Clin Res 18 (Suppl 47):17-19, 1986

11. Kjellberg RN: Proton beam therapy for arteriovenous malformation of the brain. *In* Schmidek JJ, Sweet WH (eds): Operative Neurosurgical Techniques, vol. 1. New York, Grune & Stratton, 1988, pp 911-915

12. Kjellberg RN, Hanamura T, Davis KR, et al: Bragg peak proton-beam therapy for arteriovenous malformations of the brain. N Engl J Med 309:269-274, 1983

13. Kjellberg RN, Kliman B: Lifetime effectiveness--a system of therapy for pituitary adenomas, emphasizing Bragg peak proton hypophysectomy. *In* Linfoot JA (ed): Recent Advances in the Diagnosis and Treatment of Pituitary Tumors. New York, Raven Press, 1979, pp 269-288

14. Kjellberg RN, McMeel JW, McManus NL, et al: Pituitary suppression in diabetic retinopathy by proton beam in surgically "unfit" patients. *In* Goldberg MF, Fine SL (eds): Symposium on the Treatment of Diabetic Retinopathy, Airlie House, Warrenton, VA (US Public Health Service Publication No. 1890), Arlington, 1968, pp 249-276

15. Kjellberg RN, Shintani A, Franzt AG, et al: Proton beam therapy in acromegaly. N Engl J Med 278:689-695, 1968

16. Konnov B, Melnikov L, Zargarova O, et al: Narrow proton beam therapy for intracranial lesions. *In* International Workshop on Proton and Narrow Photon Beam Therapy, Oulu, Finland, University of Oulu Printing Center, 1989, pp 48-55

17. Lawrence JH: Proton irradiation of the pituitary. Cancer 10:795-798, 1957

18. Lawrence JH: Heavy particle irradiation of intracranial lesions. *In* Wilkens RH, Rengachary SS (eds): Neurosurgery. New York, McGraw-Hill, 1985, pp 1113-1132

19. Lawrence JH, Linfoot JA: Treatment of acromegaly, Cushing disease and Nelson's syndrome. West J Med 133:197-202, 1980

20. Levy RP, Fabrikant JI, Frankel KA, et al: Stereotactic heavy-charged-particle Bragg peak radiosurgery for the treatment of intracranial arteriovenous malformations in childhood and adolescence. Neurosurgery 24:841-852, 1989

21. Levy RP, Fabrikant JI, Frankel KA, et al: Charged-particle radiosurgery of the brain. Neurosurg Clin North Am 4:955-990, 1990.

22. Levy RP, Fabrikant JI, Lyman JT, et al: Clinical results of stereotactic helium-ion radiosurgery of the pituitary gland at Lawrence Berkeley Laboratory. *In* International Workshop on Proton and Narrow Photon Beam Therapy, Oulu, Finland, 1989, pp 38-42

23. Linfoot JA: Heavy ion therapy: Alpha particle therapy of pituitary tumors. *In* Linfoot JA (ed): Recent Advances in the Diagnosis and Treatment of Pituitary Tumors. New York, Raven Press, 1979, pp 245-267

24. Luchin YeI, Minakova YeI, Krymsky VA: Proton beam irradiation of cavernous sinus meningiomas. *In* International Workshop on Proton and Narrow Photon Beam Therapy, Oulu, Finland, 1989, pp 99-100

25. Lyman JT: Complication probability as assessed from dose-volume histograms. Radiat Res 104(Suppl): S13-S19, 1985

26. Lyman JT, Chong CY: ISAH: A versatile treatment positioner for external radiation therapy. Cancer 34:12-16, 1974

27. Lyman JT, Fabrikant JI, Frankel KA: Charged-particle stereotactic radiosurgery. Nucl Instrum Methods Phys Res B10/11:1107-1110, 1985

28. Lyman, Kanstein L, Yeater F, et al: A helium-ion beam for stereotactic radiosurgery of central nervous system disorders. Med Phys 13:695-699, 1986

29. Lyman JT, Phillips MH, Frankel KA, et al: Stereotactic frame for neuroradiology and charged particle Bragg peak radiosurgery of intracranial disorders. Int J Radiat Oncol Biol Phys 16:1615-1621, 1989

30. Melnikov LA, Konnov BA, Yalnynch NN: Radiosurgery of cerebral AVM. *In* International Workshop on Proton and Narrow Photon Beam Therapy, Oulu, Finland, 1989, pp 92-98

31. Minakova YeI: Review of twenty years proton therapy clinical experience in Moscow. *In* Proceedings of the Second International Charged Particle Workshop, Loma Linda, CA, 1987, pp 1-23

32. Minakova YeI: Twenty years clinical experience of narrow proton beam therapy in Moscow. *In* Proceedings of the International Heavy Particle Therapy Workshop, Paul Scherrer Institute, Villigen, Switzerland, 1990, pp 158-162

33. Minakova YeI, Kirpatovskaya LYe, Lyass FM, et al: Proton therapy of pituitary adenomas (in Russian). Med Radiol (Mosk) 28(10):7-13, 1983

34. Minakova YeI, Krymsky VA, Luchin YeI, et al: Proton beam therapy in neurosurgical clinical practice (in Russian). Med Radiol (Mosk) 32(8):36-42, 1987

35. Minakova, YeI, Vasil'eva NN, Svyatukhina OV: Irradiation of the hypophysis with single large dose of high energy protons for advanced breast carcinoma (in Russian). Med Radiol (Mosk) 22(1):33-39, 1977

36. Phillips MH, Frankel KA, Lyman JT, et al: Heavy-charged particle stereotactic radiosurgery: Cerebral angiography and CT in the treatment of intracranial vascular malformations. Int J Radiat Oncol Biol Phys 17:419-426, 1989

37. Phillips MH, Frankel KA, Lyman JT, et al: Comparison of different radiation types and irradiation geometries in stereotactic radiosurgery. Int J Radiat Oncol Biol Phys 18:211-220, 1990

38. Phillips MH, Kessler M, Frankel KA: Image correlation of MRI, CT and cerebral angiography in the treatment planning for radiosurgery of intracranial arteriovenous malformations. Int J Radiat Oncol Biol Phys, 1990 (in press).

39. Steinberg GK, Fabrikant JI, Marks MP, et al: Stereotactic heavy-charged-particle Bragg peak radiation for intracranial arteriovenous malformations. N Engl J Med 323:96-101, 1990.

40. Tobias CA: Pituitary radiation: radiation physics and biology. *In* Linfoot JA (ed): Recent Advances in the Diagnosis and Treatment of Pituitary Tumors. New York, Raven Press, 1979, pp 221-243

41. Tobias CA, Anger HO, Lawrence JH: Radiologic use of high energy deuterons and alpha particles. Am J Roentgenol Radium Ther Nucl Med 67:1-27, 1952.

42. Tobias CA, Lawrence JH, Born JL, et al: Pituitary irradiation with high-energy proton beams: A preliminary report. Cancer Res 18:121-134, 1958.

43. Tobias CA, Roberts JE, Lawrence JH, et al: Irradiation hypophysectomy and related studies using 340-MeV protons and 190-MeV deuterons. *In* Proceedings of the International Conference on the Peaceful Uses of Atomic Energy, Geneva, 1955, pp 95-106.

44. Woodruff KH, Lyman JT, Lawrence JH, et al: Delayed sequelae of pituitary irradiation. Hum Pathol 15:48-54, 1984.

FIGURE-LEGENDS

Figure 1. The heavy-charged-particle beam profile of the 230 MeV/u (920MeV) helium-ion beam at the Lawrence Berkeley Laboratory 184-inch Synchrocyclotron at University of California at Berkeley. The beam is modified to adapt to a variety of radiological conditions. Illustrated is the unmodulated Bragg ionization curve (**left**) and its transverse profile (**right**) for stereotactic radiosurgery of an intracranial arteriovenous malformation situated at a depth of about 6 cm (*From* Fabrikant JI, Lyman JT, Frankel KA: Heavy charged-particle Bragg peak radiosurgery for intracranial vascular disorders. Radiat Res [Suppl] 104:S248, 1985; with permission.)

Figure 2. Localization radiographs and isodose contours for treatment of a pituitary adenoma with stereotactic helium-ion plateau redundancy. The isodose contours are superimposed on lateral (**left**) and anteroposterior (**right**) projections of the sella turcica, the related parasellar structures (e.g., optic chiasm and cranial nerves), and temporal lobes. Treatment used stereotactically-directed helium-ion beams, and coordinated head and trunk rotation, and was delivered in four days.

Figure 3. Diagram of charged-particle beam delivery system at the University of California at Berkeley-Lawrence Berkeley Laboratory 184-inch Synchrocyclotron used for stereotactic radiosurgery of intracranial tumors and vascular disorders. The stereotactic patient-positioning immobilization system (ISAH) allows translation along three orthogonal axes (x, y, z) and rotation about the y and z axes, thereby providing precise patient immobilization and positioning for stereotactically-directed charged-particle-beam therapy. The width of the high-dose Bragg ionization peak within the brain can be spread to the prescribed size by interposing a modulating filter of comparable maximum thickness (x cm) in the beam path. At the Bevatron accelerator, the Bragg ionization peak is modulated by use of a variable-position water column absorber. The range in tissue of the Bragg peak region is determined by a range-modifying absorber. An individually designed aperture specifically tailored to the size and configuration of the intracranial lesion shapes the beam in cross section. Tissue-equivalent compensators adjust for skull curvature and tissue inhomogeneities and further improve the precision placement of the high-dose Bragg peak region. The ion chamber monitors the dose delivered in each beam. Multiple entry angles and beamports are chosen with appropriate modifications of radiation parameters so that the high-dose regions of the individual beams intersect within the defined intracranial target with the lowest possible dose to sensitive adjacent normal brain tissues. The treatment setup illustrated is for treatment of an intracranial arteriovenous malformation and

demonstrates the integrated immobilization mask within the stereotactic frame. (*From* Levy RP, Fabrikant JI, Frankel KA, et al: Stereotactic heavy-charged-particle Bragg peak radiosurgery for the treatment of intracranial arteriovenous malformations in childhood and adolescence. Neurosurgery 24:842, 1989; with permission.)

Figure 4. MRI scans of the pituitary region of a 49-year old woman 14 years after transsphenoidal hypophysectomy for acromegaly. Recurrent tumor has resulted in endocrinologic changes associated with increased levels of growth hormone. The acromegalic tumor is identified and there is extension into the left cavernous sinus, lying directly on the left internal carotid artery. **Upper (left and right)**, Coronal views demonstrate the recurrent tumor and its relationship to the optic nerves, chiasm and tracts, left carotid artery, and adjacent cranial nerves. The tumor and cranial nerves are outlined for radiosurgical treatment planning. **Lower (left and right)**, Sagittal views demonstrate the precise distance between the upper edge of the recurrent tumor (*outlined*) and the optic chiasm (see Fig. 5) The MRI technique is part of the treatment planning procedure for stereotactic charged-particle radiosurgery. (In collaboration with C. E. Fiske.) (*From* Levy RP, Fabrikant JI, Frankel KA, et al: Charged-particle radiosurgery of the brain. Neurosurg Clin North Am 1:972, 1990; with permission.)

Figure 5. Stereotactic helium-ion Bragg peak radiosurgery treatment plan for the recurrent acromegalic tumor in the patient illustrated in Figure 4. The radiosurgical target is defined by the inner ring of white dots. The helium-ion beam was modulated 0.50 cm and collimated by a 15 x 13 mm individually shaped brass and cerrobend aperture. A dose of 30 GyE was delivered to a volume of 800 mm^3 through 8 ports in 1 day at the University of California at Berkeley-Lawrence Berkeley Laboratory Bevatron. Isodose contours are calculated for 95%, 90%, 70%, 50%, 30%, 20%, and 10% of the maximum central dose in the axial (**upper**) and coronal (**lower**) planes. The 5% isodose contour is also calculated in the coronal plane and demonstrates the rapid falloff of the radiation dose within a few millimeters of the irradiated target volume. The treatment plan was designed with an eccentric isocenter in order to place a higher dose in the tumor mass lying within the sella and a lower dose in the tumor lying against the internal carotid artery in the cavernous sinus; the optic chiasm, nerves and tracts received less than 10% of the central dose, i.e., less than 3 GyE, and the parasellar cranial nerves only a fraction of this dose. (*From* Levy RP, Fabrikant JI, Frankel KA, et al: Charged-particle radiosurgery of the brain. Neurosurg Clin North Am 1:973, 1990; with permission.)

Figure 6. The helium-ion beam path is shown in relation to the stereotactically-determined isocenter of the patient positioning system, the Irradiation Stereotactic Apparatus for

Humans (ISAH) at the medical cave at the 184-inch Synchrocyclotron at the University of California at Berkeley--Lawrence Berkeley Laboratory. The immobilization system is used for both Bragg-peak and plateau-region heavy-charged-particle radiosurgery for intracranial AVMs, pituitary tumors, and other intracranial targets. (*From* Fabrikant JI, Lyman JT, Frankel KA: Heavy charged-particle Bragg peak radiosurgery for intracranial vascular disorders. Radiat Res [Suppl] 104:S247, 1985; with permission.)

Figure 7. Stereotactic heavy-charged-particle Bragg peak radiosurgery treatment plan for a 12-year-old girl with an arteriovenous malformation of the brain stem (*inner ring of white dots*). Isodose contours have been calculated at 100%, 80%, 50%, and 10% of the maximum dose in the axial (left) and coronal (right) planes. The 100% contour conforms precisely to the periphery of the lesion. There is a very rapid fall-off in dose outside the arteriovenous malformation target volume. Since four noncoplanar beams are used, very little normal brain tissue receives even as much as 10% of the dose to the arteriovenous malformation, and most of the brain receives no radiation at all. There is virtually complete sparing and protection of midbrain and pontine structures. The helium-ion beam was collimated by an elliptical brass aperture measuring 8.5 by 11.5 mm; treatment was performed using 4 ports in 1 day, to a volume of 300 mm^3 (dose, 25 GyE). (*From* Levy RP, Fabrikant JI, Frankel KA, et al: Stereotactic heavy-charged-particle Bragg peak radiosurgery for the treatment of intracranial arteriovenous malformations in childhood and adolescence. Neurosurgery 24:843, 1989; with permission.)

Figure 8. Stereotactic helium-ion Bragg peak radiosurgery treatment plan for a large right frontal AVM. The helium-ion beam was collimated by individually-shaped brass and cerrobend apertures measuring 47 x 35 mm and 49 x 37 mm A dose of 28 GyE was delivered to the AVM (*inner ring of white dots*) using 5 ports in 2 days to a volume of 26,000 mm^3. Isodose contours in the axial plane are calculated for 10, 30, 50, 80, and 90% of the maximum dose. The 90% contour borders precisely on the periphery of the lesion. Note the rapid dose fall-off to the 80 % level, and that the 10% isodose contour completely spares and protects the contralateral hemisphere. (*From* Levy RP, Fabrikant JI, Frankel KA, et al: Stereotactic heavy-charged-particle Bragg peak radiosurgery for the treatment of intracranial arteriovenous malformations in childhood and adolescence. Neurosurgery 24:847, 1989; with permission.)

Figure 9. Stereotactic cerebral angiograms of a 39-year-old man presenting with recurrent seizures from a large (54,000 mm^3) left hemisheric cerebral AVM. Upper, lateral left internal carotid artery (left) and vertebral artery (right) angiograms demonstrate the size, shape and location of the AVM which is supplied by branches of the left middle cerebral

and vertebral arteries. The vascular steal is pronounced, and the entire ipsilateral cortex is underperfused. **Lower**, lateral left carotid artery (**left**) and vertebral artery (**right**) angiograms during the first followup cerebral angiogram 12 months after stereotactic heavy-charged-particle Bragg peak radiosurgery (dose, 27 GyE) demonstrate complete obliteration of the malformation. The vascular steal has been reversed, and normal or near-normal hemodynamic conditions have been restored. (*From* Fabrikant JI, Levy RP, Steinberg GK, et al: Charged-particle radiosurgery for intracranial vascular malformations. Neurosurg Clin North Am, 1990, in press; with permission.)

Figure 10. Positron emission tomography (PET) scan and magnetic resonance image (MRI) of a 35-year-old man with a large left frontoparietal arteriovenous malformation 24 months following heavy charged-particle radiosurgery (helium ions; dose, 35 GyE). *A*, Marked depression of glucose metabolism in the left parietal cortex is demonstrated on ^{18}fluorodeoxyglucose PET scan (taken with the Donner Laboratory 600 crystal high-resolution scanner). *B*, The corresponding MRI scan shows intense white matter signal in the same area; the changes are associated with profound vasogenic edema. The patient was clinically normal at this time but 18 months later developed mild right-sided hemiparesis with clumsiness of hand and foot function and diminished mentation. Gadolinium-MRI scans suggested a possible underlying etiology of radiation necrosis, and surgical exploration identified a well-defined region of radiation necrosis. The arteriovenous malformation was thrombosed, and part of the thrombosed vascular mass was removed. The patient has improved clinically and has returned to work. (*From* Valk PE, Dillon WP: Diagnostic imaging of central nervous system radiation injury. *In* Gutin PH, Leibel SA, Sheline GE (eds): Radiation Injury to the Nervous System. New York, Raven Press, 1990, in press; with permission).

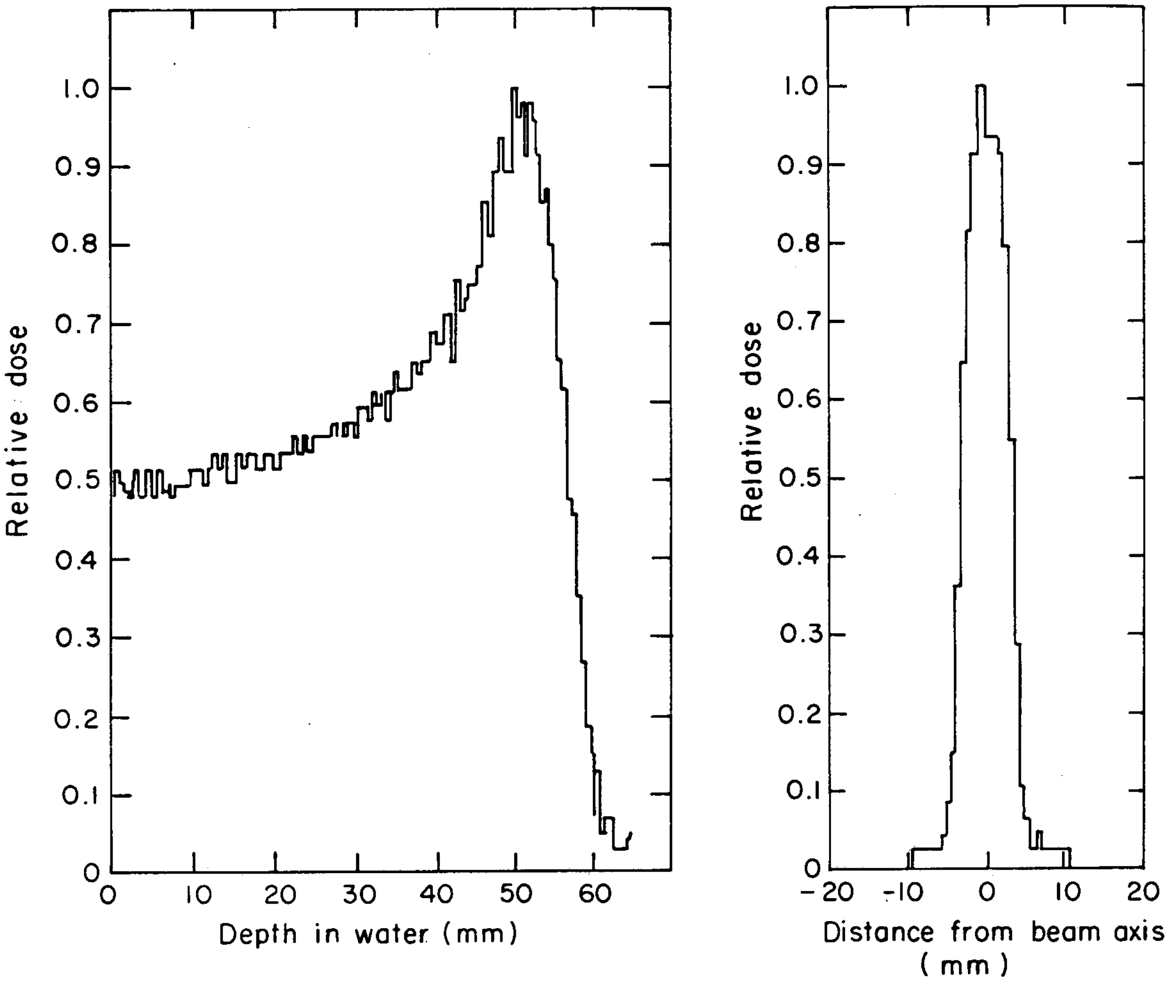

XBL 828 – 1107

Figure 1

XBB 780-15500

Figure 2

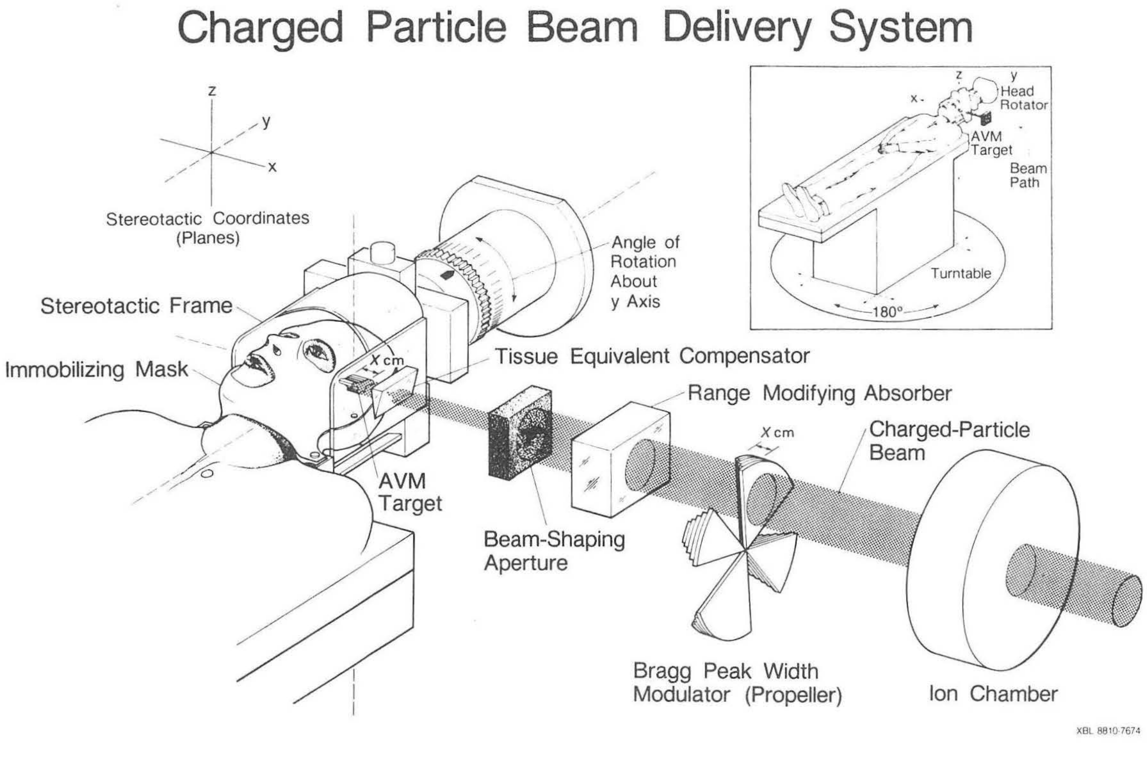
Charged Particle Beam Delivery System
z
y
x
Stereotactic Coordinates (Planes)
Stereotactic Frame
Immobilizing Mask
X cm
AVM Target
Angle of Rotation About y Axis
Tissue Equivalent Compensator
Range Modifying Absorber
X cm
Charged-Particle Beam
Beam-Shaping Aperture
Bragg Peak Width Modulator (Propeller)
Ion Chamber
z
y
x
Head Rotator
AVM Target
Beam Path
Turntable
180°
XBL 8810-7674

Figure 3

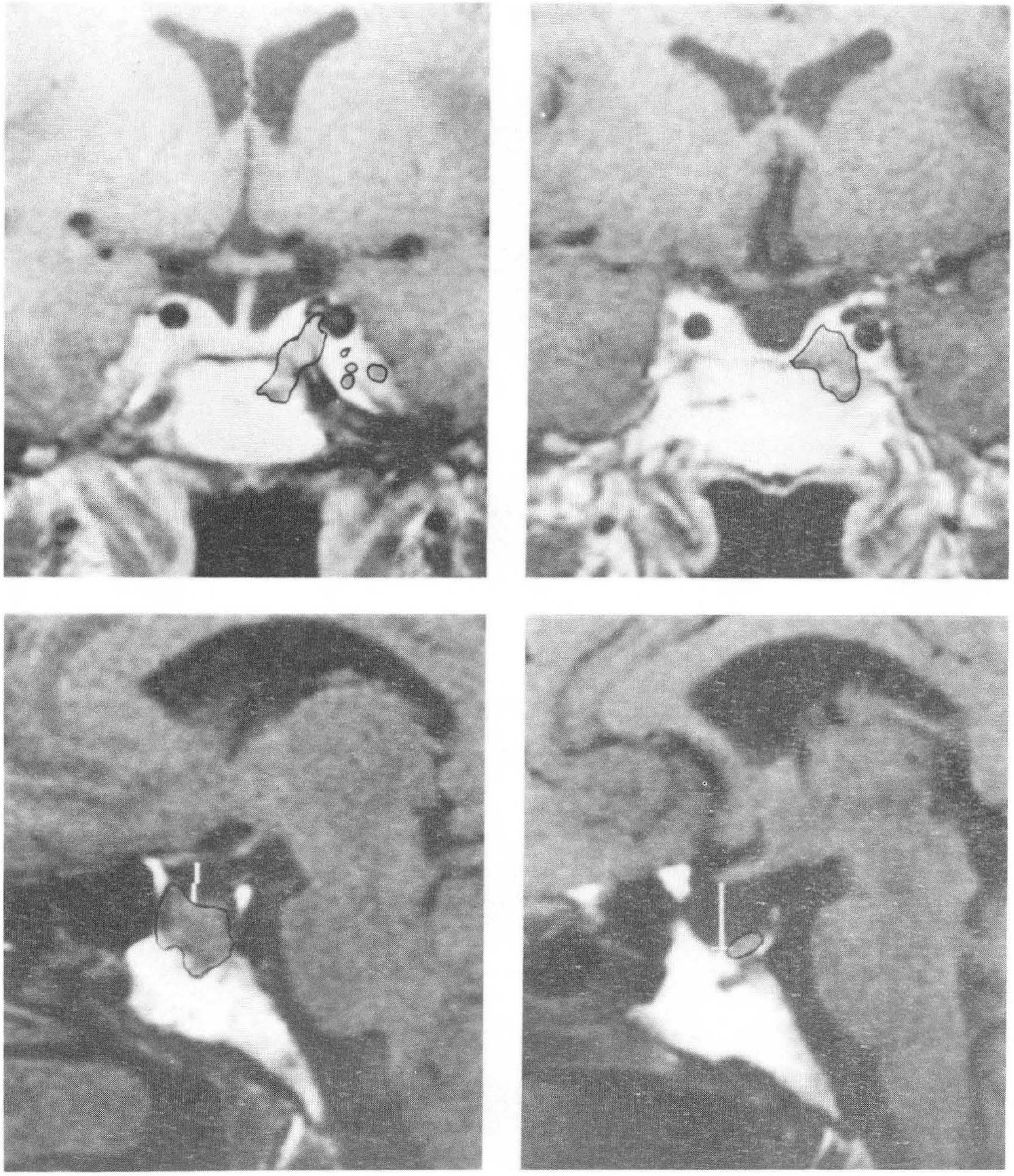

XBB 898-6688A

Figure 4

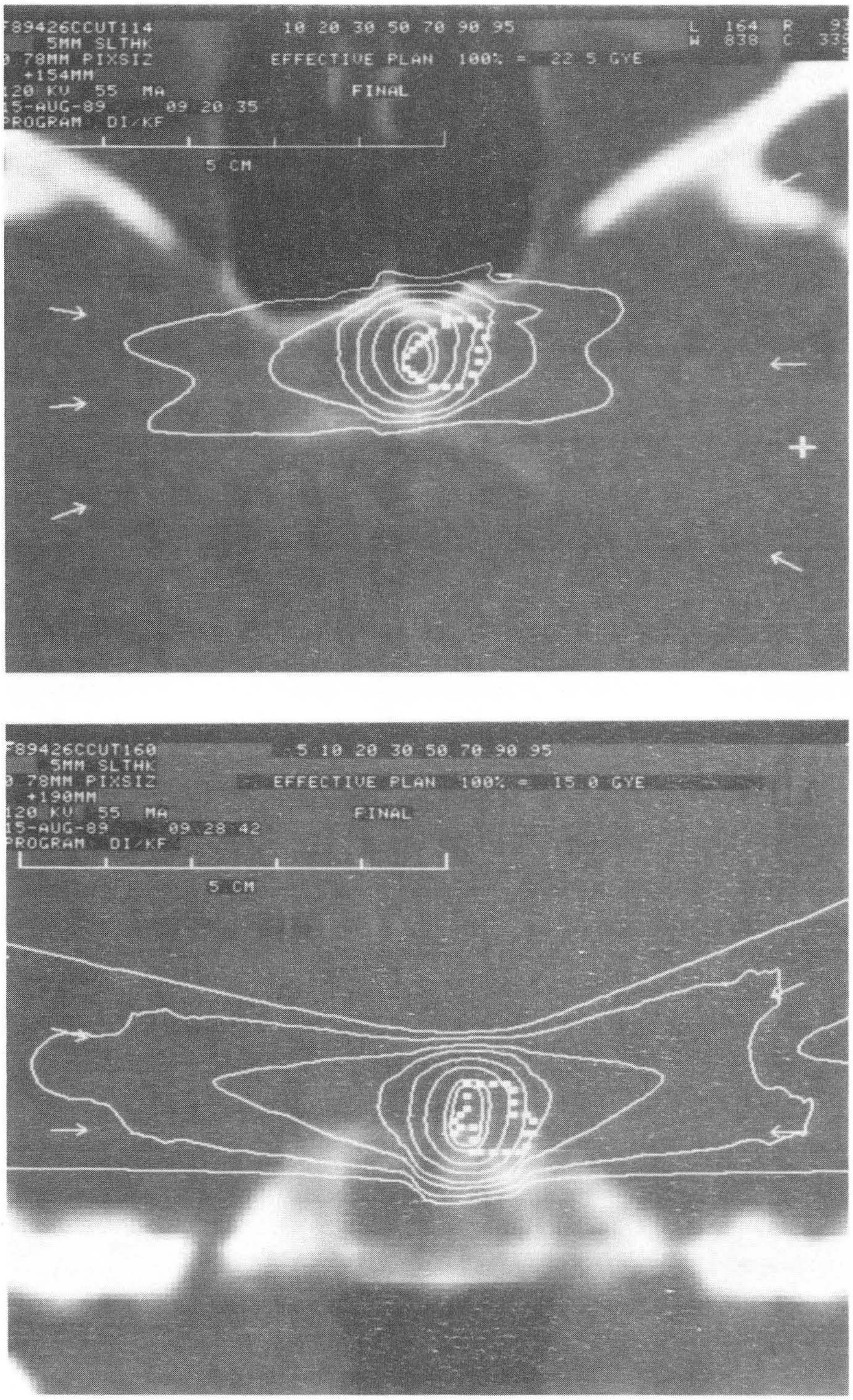

XBB 898-6680

Figure 5

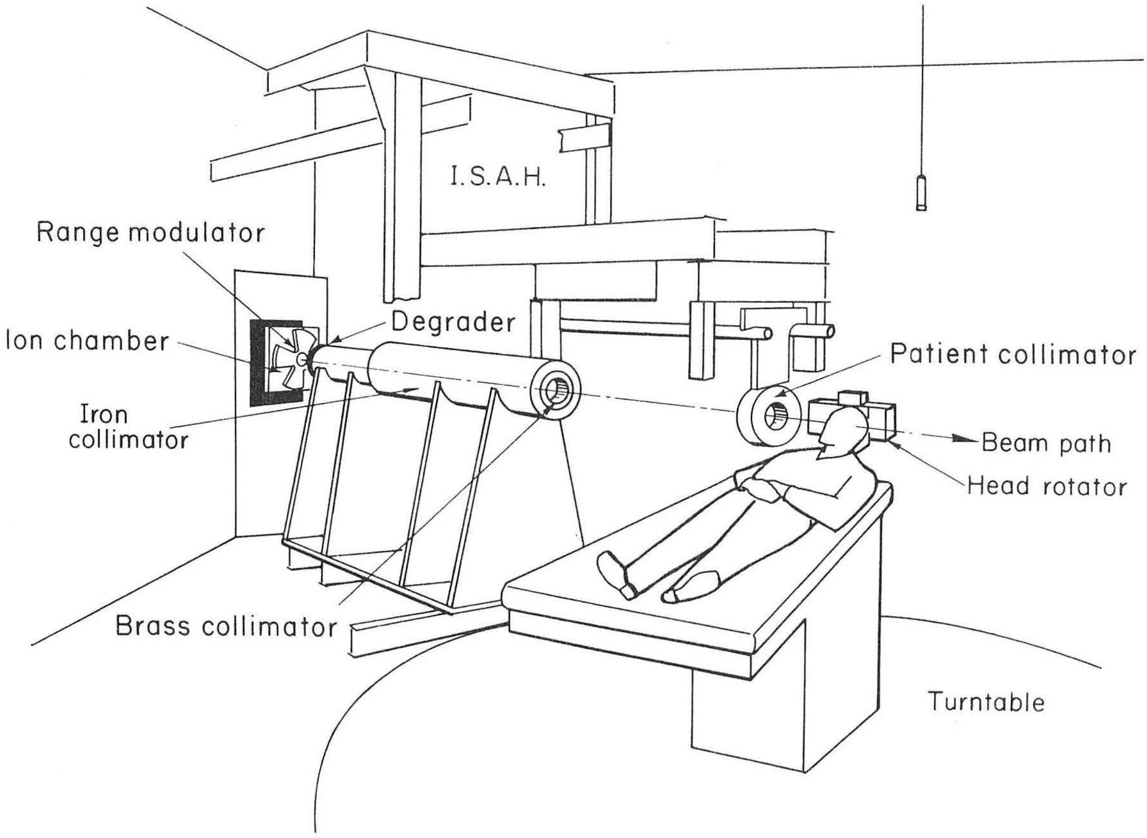
I.S.A.H.
Range modulator
Ion chamber
Degrader
Iron collimator
Patient collimator
Beam path
Head rotator
Brass collimator
Turntable
XBL 824-486

Figure 6

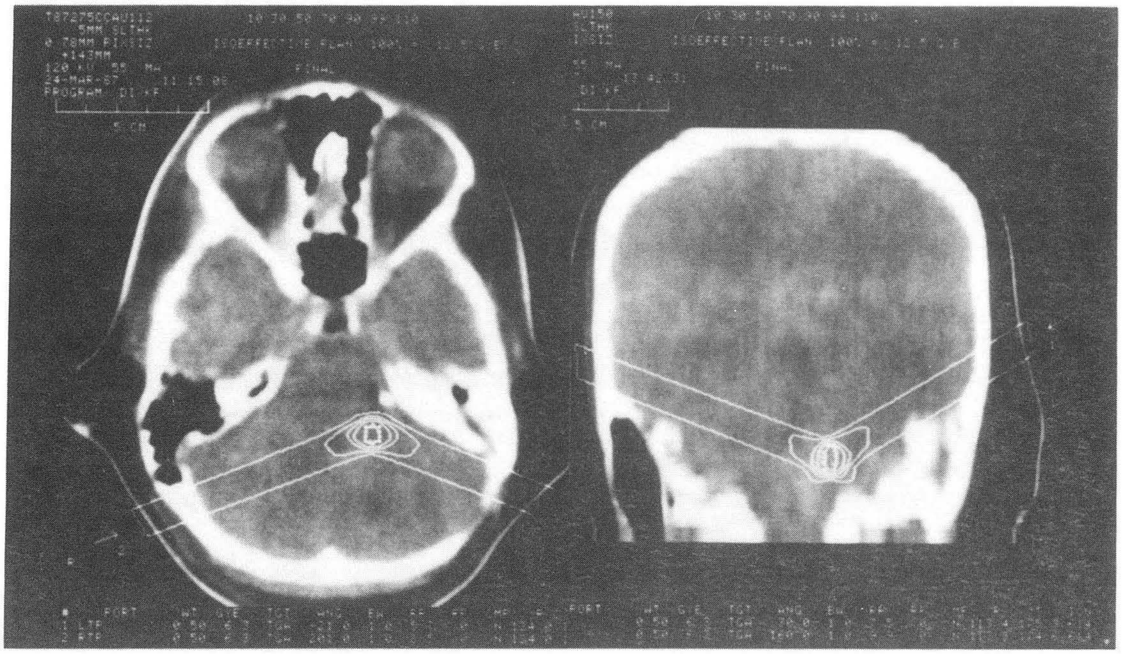

XBB 916-4302A

Figure 7

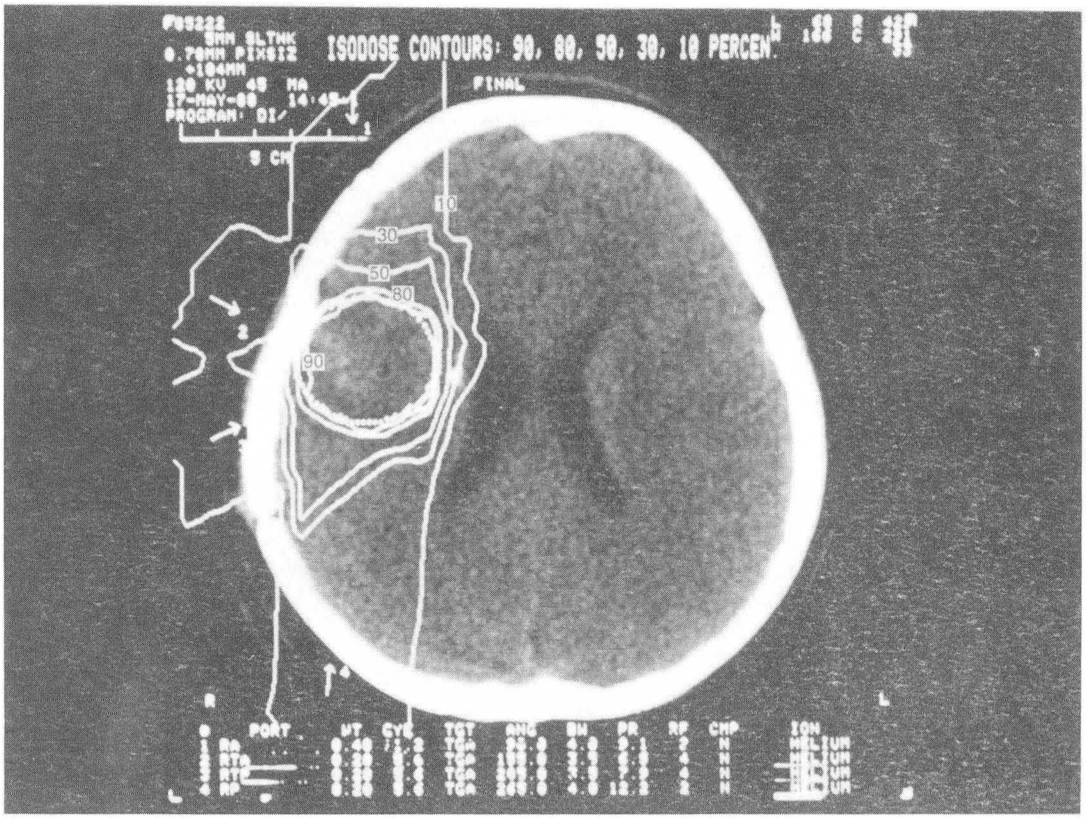

XBB 885-5363A

Figure 8

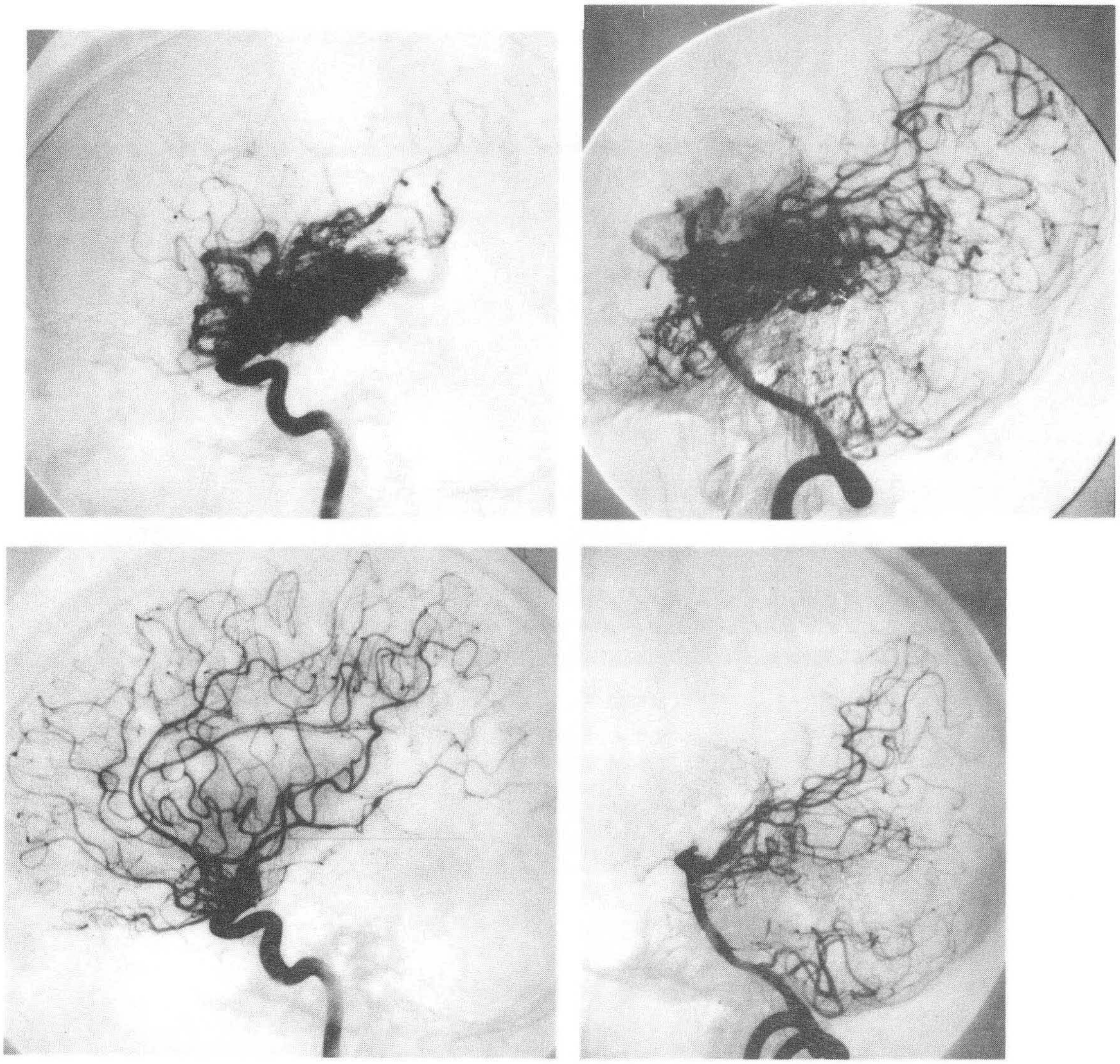

XBB 876-5281

Figure 9

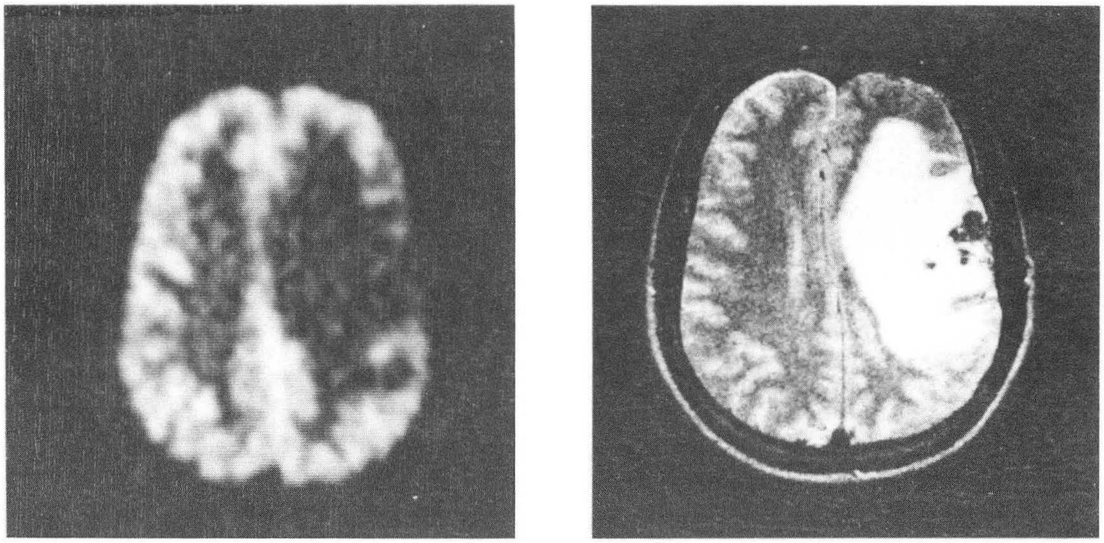

XBB 887-7044

Figure 10

LAWRENCE BERKELEY LABORATORY
TECHNICAL INFORMATION DEPARTMENT
1 CYCLOTRON ROAD
BERKELEY, CALIFORNIA 94720